Mixed-order phase transition in a two-step contagion model with single infectious seed

Wonjun Choi,[1] Deokjae Lee,[1] and B. Kahng[1,*]

[1] *CCSS, CTP and Department of Physics and Astronomy, Seoul National University, Seoul 08826, Korea*

(Dated: December 4, 2016)

Percolation is known as one of the most robust continuous transitions, because its occupation rule is intrinsically local. As one of the ways to break the robustness, occupation is allowed to more than one species of particles and they are cooperatively occupied. This generalized percolation model undergoes a discontinuous transition. Here we investigate an epidemic model with two contagion steps and characterize its phase transition analytically and numerically. We find that even though the order parameter jumps at a transition point r_c, then increases continuously, it does not exhibit any critical behavior: the fluctuations of the order parameter do not diverge at r_c. However, critical behavior appears in mean outbreak size, which diverges at the transition point in a manner that the ordinary percolation shows. Such a type of phase transition is regarded as a mixed-order phase transition. We also obtain scaling relations of cascade outbreak statistics when the order parameter jumps at r_c.

PACS numbers: 89.75.Hc, 64.60.ah, 05.10.-a

I. INTRODUCTION

Percolation [1] has long served as a model for the formation of a giant cluster ranging from gelation in polymers to opinion formation in society. Percolation transitions based on ordinary percolations are continuous, whereas abrupt percolation transitions are often observed in real-world complex systems. Recently, considerable efforts have been made to generate discontinuous percolation transitions, coming to the conclusion that a discontinuous percolation transition cannot occur unless its occupation rule is nonlocal [2, 3].

Alternatively, when more than one species of particles cooperatively occupy each node, a discontinuous percolation transition can occur even though the dynamic rule is local [4, 5]. Along this line, we first consider a SIR model in which a node is one of three states, susceptible (S), infected (I) and recovered (R) states. A node in I state transfers pathogen to each susceptible neighbor with rate κ, then it is recovered with rate λ. When the epidemic dynamics starts from single infected node, the spread of infected (eventually recovered) nodes can be regarded as the growth of a cluster in percolation [6–8].

A generalized epidemic model from the SIR model was proposed in Refs. [9, 10], which allows the occupation of double pathogens $\mathrm{I_a}$ and $\mathrm{I_b}$ on each node instead of single pathogen I. Once a node has been infected by one type of pathogen, it can be more easily infected by the other type of pathogen, which leads to a discontinuous transition. A similar epidemic model was proposed (called the SWIR model) on regular lattice [11] and on random graph [12], which is another generalization of the SIR model by allowing an intermediate state W called the weakened state (W) between susceptible state (S) and infectious state (I). Thus, the SWIR model contains the reactions: $S + I \to 2I$, $S + I \to W + I$, $W + I \to 2I$ and $I \to R$. Those reactions occur with rates κ, μ, ν and λ, respectively. A node in state W becomes more easily infected than a node in state S, which leads to a discontinuous transition. Original studies of the SWIR contagion models focused on the behavior of the order parameter, the fraction of nodes in state R as a function of a control parameter, the set of epidemic rates. To understand critical behavior thoroughly, one needs to check diverging behaviors of the susceptibility and correlation length as well. In this paper, we aim to understand thoroughly nature of the phase transition and critical phenomena of this SWIR model with single seed on the Erdős and Rényi (ER) networks [13]. We find that the transition is of mixed-order under a certain condition: while the order parameter jumps discontinuously, some physical quantities show the critical behavior of the SIR model, feature of a continuous transition.

The critical behavior appears in the following manner: finite outbreaks occur and their sizes are heterogeneous following a power-law distribution $p_s(r) \sim s^{-\tau_a} \exp(-s/s^*)$, where $\tau_a = 3/2$ and $s^* \sim (r - r_c)^{-1/\sigma_a}$ with r_c being a transition point. Mean size of finite outbreaks diverges as $\chi_a \equiv \sum_s s p_s(r) \sim (r - r_c)^{-\gamma_a}$. Using finite size scaling analysis, we determine the critical exponents $\{\gamma_a, \bar{\nu}_a\}$, where $\bar{\nu}_a$ is the exponent defined in the relation $\chi_a \sim N^{\gamma_a/\bar{\nu}_a}$ at a transition point in finite systems. Moreover, we investigate various properties of cascade outbreak dynamics.

The probability P_∞ that a macroscopic-scale outbreak (called an infinite outbreak hereafter) exhibits a continuous phase transition as in the model [10]. An infinite outbreak is required for the order parameter to jump from zero to a finite value. It was shown [14] that in the SWIR model the probability $P_\infty(r)$ is nothing but the spanning probability of the percolation. Thus, we show that the set of exponents $\{\gamma_a, \sigma_a, \bar{\nu}_a\}$ reduces to the critical exponents of the ordinary percolation $\{\gamma_p, \sigma_p, \bar{\nu}_p\}$ as that of the SIR model is.

* bkahng@snu.ac.kr

The SWIR model exhibits rich phase transition behaviors such as tricritical behavior and so on. We obtain the critical exponents related to the order parameter and cascade outbreak dynamics analytically and numerically and confirm previously obtained results [14].

The paper is organized as follows: In Sec. II, we present the SWIR model. In Sec. III, we set up the self-consistency equation to derive the mean-field solution of the order parameter for the epidemic transition on the Erdős and Rényi (ER) networks. We find that depending on the mean degree of the ER network, different types of phase transition can occur. In Sec. IV, we investigate the properties of those diverse phase transitions. In the final section, a summary and discussion are presented.

II. THE SWIR MODEL

We first define the reactions of the SWIR model as follows:

$$\mathrm{S} + \mathrm{I} \xrightarrow{\kappa} \mathrm{I} + \mathrm{I}, \tag{1}$$

$$\mathrm{S} + \mathrm{I} \xrightarrow{\mu} \mathrm{W} + \mathrm{I}, \tag{2}$$

$$\mathrm{W} + \mathrm{I} \xrightarrow{\nu} \mathrm{I} + \mathrm{I}, \tag{3}$$

$$\mathrm{I} \xrightarrow{\lambda} \mathrm{R}, \tag{4}$$

where κ, μ, ν and λ denote the reaction rates of the respective reactions between the states of neighboring nodes. A node in state S can change its state when it contacts with a node in state I to either state I via reaction (1) with a probability $\kappa/(\kappa+\mu+\lambda)$ or via successive two reactions (2) and (3) with a probability rw where $r = \mu/(\kappa+\mu+\lambda)$ and $w = \nu/(\nu+\lambda)$ are the reaction probability for (2) and (3). The node can also change its state to W with a probability $r(1-w)$. Detail explanations for the reaction probabilities are in Appendix A. The main issue of this SWIR model is to determine how fast disease spreads on a macroscopic scale with respect to the recovery rate λ. Thus, without loss of generality, we set $\lambda = 1$. On the other hand, when μ and ν are much smaller than κ, the model reduces to the SIR model. Thus, we focus on the opposite limit: the reaction rates of (2) and (3) are dominant compared with that of (1). Thus, we set $\kappa = 0$ and $\nu = 1$ for simplicity. Thus, $w = 1/2$. The reaction rate μ serves as a control parameter. For convenience, we will use $r \equiv \mu/(1+\mu)$ as the control parameter.

Initially, there exist a single infectious node (seed), the location of which is chosen at random and $N-1$ susceptible nodes. We then successively choose which reaction will occur next and when it will occur. The simulation rule is presented in Appendix A. This process is repeated until no infectious nodes remain in the system. This state is called absorbing state [15]. Here we are interested in the behavior of the outbreak size of epidemics, i.e., the fraction of nodes in state R after the system reaches an absorbing state, which serves as the order parameter, denoted as m. Moreover, the susceptibility, i.e., the fluctuations of the order parameter defined as $\chi_m \equiv N(\langle m^2\rangle - \langle m\rangle^2)$ averaged over the ensemble is considered as a function of r. Using finite-size scaling analysis, we will study phase transitions.

III. SELF-CONSISTENCY EQUATION AND PHYSICAL SOLUTIONS

In an absorbing state, each node is in one of three states, the susceptible S, weakened W and recovered R states. The order parameter $m(r)$, the fraction of nodes in state R in an absorbing state, is written as

$$m(r) = \sum_{k=1}^{\infty} P_d(k) \sum_{\ell=1}^{k} \binom{k}{\ell} q^{\ell}(1-q)^{k-\ell} P_R(\ell), \tag{5}$$

where $P_d(k)$ is the probability that a randomly selected node has degree k. q is the probability that an arbitrarily chosen edge leads to a node in state R but not infected through the chosen edge in the absorbing state. $P_d(k)\binom{k}{\ell}q^k(1-q)^{k-\ell}$ is the probability that a node has degree k, among which ℓ neighbor nodes are in state R in the absorbing state. $P_R(\ell)$ is the conditional probability that a node is finally in state R, provided that its ℓ neighbors are in state R in the absorbing state.

Similarly to $P_R(\ell)$, we present $P_S(\ell)$ as the conditional probability that a node remains in state S in the absorbing state, provided that it has ℓ neighbors in state R. $P_W(\ell)$ can be described similarly. We note that for a certain node to have ℓ neighbors in R state in the absorbing state means that the node received attempts from those ℓ recovered neighbors when they were in state I. Thus, a node that still remains in state S with ℓ neighbors in state R has been uninfected by ℓ attempts of infection through the whole process. Thus we obtain

$$P_{\mathrm{S}}(\ell) = (1-r)^{\ell}. \tag{6}$$

Next, the probability $P_{\mathrm{W}}(\ell)$ is given as

$$P_{\mathrm{W}}(\ell) = \sum_{j=0}^{\ell-1} (1-r)^j r (1-w)^{\ell-j}, \tag{7}$$

where j denotes the number of attacks that a node received but sustains before it changes to state W. Using the relation $P_{\mathrm{S}}(\ell)+P_{\mathrm{W}}(\ell)+P_{\mathrm{R}}(\ell) = 1$, one can determine $P_{\mathrm{R}}(\ell)$ in terms of P_{S} and P_{W}.

Local tree approximation allows us to define q_n similarly to q but now at the tree level n. The probability q_{n+1} can be derived from q_n as follows:

$$\begin{aligned} q_{n+1} &= \sum_{k=2}^{\infty} \frac{k P_d(k)}{\langle k\rangle} \sum_{\ell=1}^{k-1} \binom{k-1}{\ell} q_n^{\ell}(1-q_n)^{k-1-\ell} P_{\mathrm{R}}(\ell) \\ &\equiv f(q_n), \end{aligned} \tag{8}$$

where the factor $kP_d(k)/\langle k\rangle$ is the probability that a node connected to a randomly chosen edge has degree k. As a particular case, when the network is an ER network having a degree distribution that follows the Poisson distribution, i.e., $P_d(k) = \langle k\rangle^k e^{-\langle k\rangle}/k!$, where $\langle k\rangle = \sum_k kP_d(k)$ is the mean degree, the function $f(q_n)$ is reduced as follows:

$$f(q_n) = 1 - e^{-rq_n\langle k\rangle} + \frac{r}{1-2r}e^{-q_n\langle k\rangle/2} - \frac{r}{1-2r}e^{-rq_n\langle k\rangle}. \tag{9}$$

Eq. (8) reduces to a self-consistency equation for q for a given reaction probability r in the limit $n \to \infty$. Once we obtain the solution of q, we can obtain the outbreak size $m(r)$ using Eq. (5). For ER networks, however, $m(r)$ becomes equivalent to q so that the solution of the self-consistency equation Eq. (8) yields the order parameter. We remark that the method we used is similar conceptually to those used in previous studies of epidemic spreading on complex networks [4, 12, 14, 16–18].

For convenience, we define a function $G(m) \equiv f(m) - m$. Using formula (9), we approximate $G(m)$ in the limit $m \to 0$ as

$$G(m) = am + bm^2 + cm^3 + O(m^4), \tag{10}$$

where

$$a = \frac{1}{2}(r - r_a)\langle k\rangle, \tag{11}$$

$$b = \frac{1}{4}r(r_b - r)\langle k\rangle^2, \tag{12}$$

$$c = \frac{1}{12}r(r - r_c^+)(r - r_c^-)\langle k\rangle^3 \tag{13}$$

with $r_a = 2/\langle k\rangle$, $r_b = 1/2$ and $r_c^\pm = (1 \pm \sqrt{5})/4$. Because $r_c^- < 0$, c can change sign only across r_c^+ in the range $0 < r_c^+ < 1$. However, because $G(m) \to -\infty$ as $q \to \infty$, we limit our investigation to the range $r < r_c^+$ hereafter, so that c is always negative. For convenience, we neglect the higher order terms and redefine $G(m)$ as

$$G(m) = am + bm^2 + cm^3. \tag{14}$$

Depending on the relative magnitude between a and b, various solutions of the self-consistency equation $G(m) = 0$ can exist. However, we need to check whether those solutions are indeed physically relevant in the steady state when we start epidemic dynamics from the given initial condition. We set up the stability criterion as follows: We impose a small perturbation to the steady state solution q^* of Eq. (8). Then we can obtain the recursive equation as

$$q^* + \delta q_{n+1} \approx f(q^*) + \frac{df}{dq}\Big|_{q=q^*}\delta q_n, \tag{15}$$

which leads to

$$\eta \equiv \frac{\delta q_{n+1}}{\delta q_n} = \frac{df}{dq}\Big|_{q=q^*}. \tag{16}$$

If $\eta < 1$ (> 1), then the steady state solution q^* is stable (unstable).

IV. PHASE TRANSITIONS

We investigate diverse types of phase trasitions. The equation of state in the steady state can be obtained using $G(m) = 0$. From Eq. (14), there exist one trivial solution $m = 0$ and two non-trivial solutions $m = m_d$ and m_u, where

$$m_d(r) = -\frac{b}{2c} - \sqrt{\frac{b^2}{4c^2} - \frac{a}{c}}, \tag{17}$$

$$m_u(r) = -\frac{b}{2c} + \sqrt{\frac{b^2}{4c^2} - \frac{a}{c}}. \tag{18}$$

Particularly, when $b^2 - 4ac = 0$, $m_d = m_u$, which is denoted as m_*. Depending on the relative magnitude between $r_a = 2/\langle k\rangle$ and $r_b = 1/2$, which determines the signs of a and b, diverse types of non-trivial solutions of $G(m) = 0$ exist. For the order parameter to jump discontinuously at the transition point, $r_a < r_b$ must be satisfied [4]. Thus, we consider three cases depending on relative magnitude between $\langle k\rangle$ and $k_c = 4$: i) When $\langle k\rangle > 4$, a mixed-order transition occurs. ii) When $\langle k\rangle = 4$, a tricritical transition occurs. iii) When $\langle k\rangle < 4$, a continuous transition occurs. For each case, the critical exponent of the order parameter is determined analytically, which is presented in Appendix B. We also perform extensive numerical simulations to support the analytic solution and to see various critical behaviors. In all simulations, $\kappa = 0$ and $\nu = 1$ are used. ER networks of mean degree $\langle k\rangle = 3, 4$, and 8 are used. Ensemble average is taken over more than 2×10^4 samples for each set of parameter values.

A. For $\langle k\rangle > 4$

When $\langle k\rangle > 4$, $r_a < r_b$. The behavior of $G(m)$ as a function of m is schematically shown in Fig. 1 and the solution m of $G(m) = 0$ as a function of r is schematically shown in Fig. 2. There are several mathematical solutions: the physically relevant solution of the order parameter is indicated by solid line for $r < r_a$ and by solid curve for $r > r_a$. At r_a, the order parameter jumps to the extent of $m(r_a)$. The details are described as follows:

i) For $r < r_* < r_a$, there exists one stable solution $m = 0$. Recall that r_* is the solution of the equation $b^2 - 4ac = 0$.

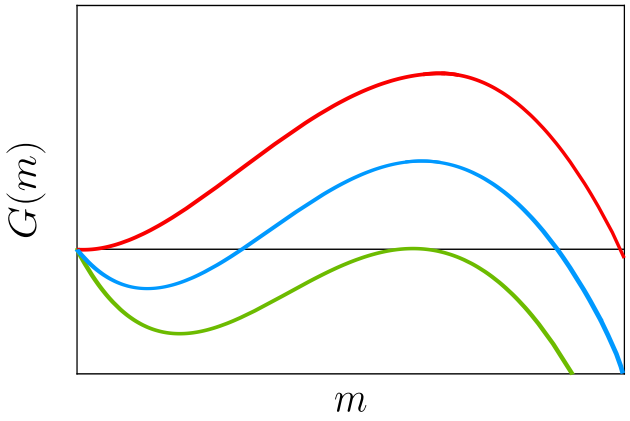

FIG. 1. For $\langle k\rangle > 4$, schematic plot of $G(m)$ versus m for fixed reaction probabilities $r = r_*$ (bottom, green), $r_* < r < r_a$ (middle, blue), and $r = r_a$ (top, red). $G(m)$ becomes zero at $m = 0$, m_d and m_u, which are determined using Eqs. (17) and (18)

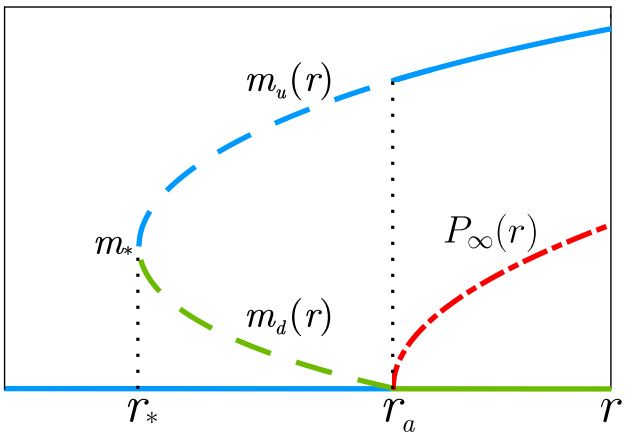

FIG. 2. Schematic plot of $m(r)$ for $\langle k\rangle > 4$. Stable solutions of $m(r)$ are represented by blue (solid or dashed) curve and line, whereas unstable solutions are done by green (solid or dashed) curve and line. Physically accessible states are indicated by solid lines, whereas inaccessible states are indicated by dashed lines. The probability $P_\infty(r)$ is indicated by dashed-dotted curve. The order parameter $m(r)$ jumps from $m = 0$ to $m_u(r)$ at r_a with the probability $P_\infty(r)$.

ii) At $r = r_* < r_a$, there exist one trivial solution $m = 0$ and one nontrivial solution $m = m_* > 0$, where $m_* = -b/(2c)$. The solution m_* is not accessible in the thermodynamic limit because there exists one stable solution $m = 0$. The probability $P_\infty(r)$ that an infinite outbreak occurs in a given sample is zero in the thermodynamic limit. However, in finite systems, the probability $P_{\infty,N}(r)$ that an outbreak of size $O(N)$ occurs can be nonzero even for $r < r_a$ (see Fig. 7). Thus, the solution $m = m_*$ could be barely observed in finite systems.

iii) When $r_* < r < r_a$, there exist one trivial and stable solution $m = 0$ and two nontrivial solutions $m_d(r)$ and $m_u(r)$. The solution m_d is unstable but m_u is stable. Because the initial density of infectious seeds is zero and $P_\infty(r) = 0$ in this interval, the solution m_u is inaccessible and unphysical. However, in finite systems, the order parameter can have the solution $m_u(r)$ with the probability $P_{\infty,N}(r)$ (see Fig. 7).

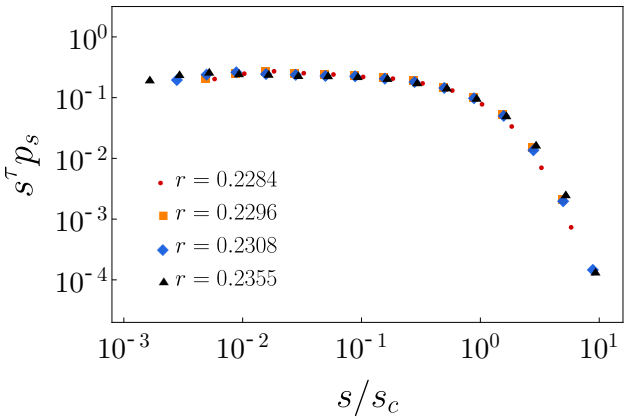

FIG. 3. Scaling plot of the outbreak size distribution $s^{\tau_a} p_s(r)$ versus s/s_c for several values of $r < r_a$, in which $\tau_a = 1.5$ and $s_c \sim (r_a - r)^{-1/\sigma_a}$ with $\sigma_a = 0.5$ are used. Data are obtained from systems of $N = 5.12 \times 10^6$ and $\langle k\rangle = 8$.

iv) At $r = r_a$, there exist one trivial solution $m = 0$ and one nontrivial solution $m = m_u$ as the case iii). Finite and infinite outbreaks can occur. From the numerical data, we find that the size distribution of finite outbreaks around r_a follows a power law with an exponential cutoff as $p_s(r) \sim s^{-\tau_a}\exp(-s/s_c)$, where $\tau_a \approx 1.5$ and $s_c \sim |r - r_a|^{-1/\sigma_a}$ with $\sigma_a \approx 0.5$ (Fig. 3). The mean size $\langle s\rangle$ of finite outbreaks exhibits a diverging behavior, which is another susceptibility defined as $\chi_a \equiv \langle s\rangle = \sum' s p_s$, where the prime indicates that the summation runs over finite clusters, as $\sim (r_a - r)^{-\gamma_a}$. From the scaling relation, it follows that $\gamma_a = (2-\tau_a)/\sigma_a \approx 1$. In finite systems, the susceptibility diverges as $\chi_a \sim N^{\gamma_a/\bar{\nu}_a} g(|r - r_a|N^{1/\bar{\nu}_a})$ (Fig. 4), where $\bar{\nu}_a$ is the exponent associated with the correlation size of finite outbreaks, defined as $\bar{\nu}_a = d_u \nu_a$ with d_u is the upper critical dimension $d_u = 6$ and ν_a is the correlation length exponent. We confirm that the measured value γ_a satisfies the scaling relation $\gamma_a = (2 - \tau_a)/\sigma_a$. The exponent $\bar{\nu}_a \approx 3$ is obtained. However, $\chi_m(r_a)$ does not diverge. The probability $P_\infty(r_a) = 0$ but $P_{\infty,N}(r_a) \neq 0$ in finite systems. Thus there can exist infinite outbreaks of size $Nm_u(r_a)$ with the probability $P_{\infty,N}(r_a)$ in finite systems.

v) For $r > r_a$, there exist one unstable solution $m = 0$ and one stable nontrivial solution $m = m_u$. Thus, the system can be in pandemic state to the extent of $m = m_u$ with the probability $P_\infty(r)$. With the remaining probability $1 - P_\infty(r)$, the system remains in the state $m = 0$. The probability $P_\infty(r)$ is equivalent to the spanning probability of percolation [10, 14, 19], which is given as $\sim (r - r_a)^{\beta_p}$, where β_p is the exponent for the order

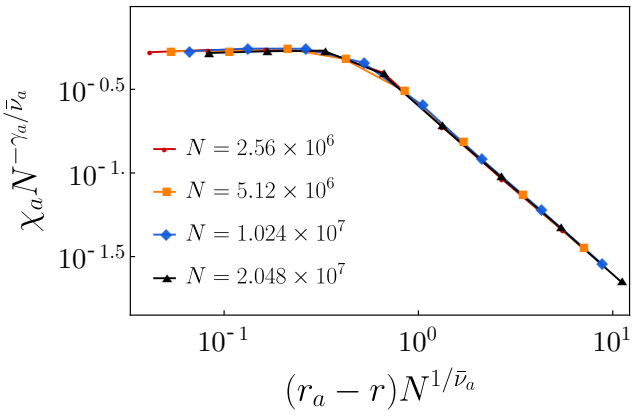

FIG. 4. Scaling plot of the susceptibility χ_a versus the reaction probability $r < r_a$ in the form $\chi_a N^{-\gamma_a/\bar{\nu}_a}$ and $(r_a - r)N^{1/\bar{\nu}_a}$, respectively. Data are obtained from systems of different system sizes N but with the same mean degree $\langle k \rangle = 8$. With the choice of $\gamma_a = 1$ and $\bar{\nu}_a = 3$, data from different system sizes are well collapsed onto a single curve.

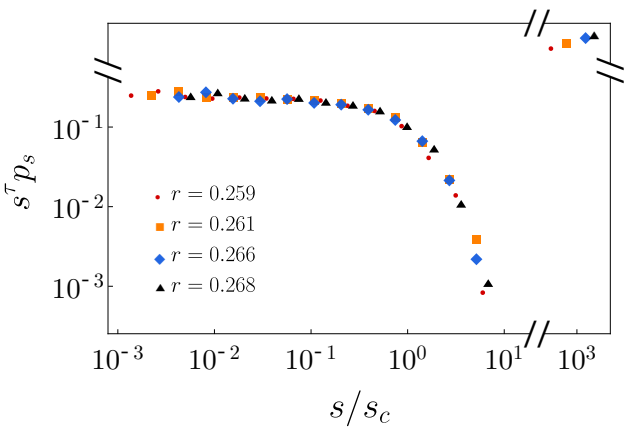

FIG. 5. Scaling plots of the outbreak size distribution versus s for several values of $r > r_a$, in which $\tau_a = 1.5$ and $s_c \sim (r - r_a)^{-1/\sigma_a}$ with $\sigma_a = 0.5$ are used. Data of macroscopic-scale outbreak sizes appear away from the curves of finite outbreaks. Data are obtained from systems of $N = 5.12 \times 10^6$ with $\langle k \rangle = 8$.

parameter of the ordinary percolation transition, which is known as $\beta_p = 1$ for ER networks. When an infinite outbreak occurs, the order parameter $m(r)$ behaves as $m(r) - m_u(r_a) \sim (r - r_a)$. However, the susceptibilities χ_m both at both $(r_a, 0)$ and $(r_a, m_u(r_a))$ do not diverge. Critical behavior of χ_a occurs at $(r, m) = (r_a, 0)$ owing to the singular behavior of $P_\infty(r)$.

In finite systems, the distribution of finite outbreak sizes for $r > r_a$ is similar to that for $r < r_a$ as $p_s(r) \sim s^{-\tau_a} \exp(-s/s_c)$, where $\tau_a \approx 1.5$ and $s_c \sim (r - r_a)^{-1/\sigma_a}$ with $\sigma_a \approx 0.5$ (Fig. 5). The mean size $\langle s \rangle$ of finite outbreaks exhibits a scaling behavior, which is the susceptibility $\chi_a \equiv \langle s \rangle = \sum' s p_s$, as $\sim N^{\gamma_a/\bar{\nu}_a}$ (Fig. 6). It turns out to be that $\bar{\nu}_a = \bar{\nu}_p$, where $\bar{\nu}_p$ is the exponent associated with the correlation size of percolation.

Here we discuss finite-size scaling behavior. We choose $\langle k \rangle = 8$ for simulations, thus the transition point is located at $r_a = 1/4$. In Fig. 7(a), we examine the probability $p(m)$ that at a certain $r = 0.2754 > r_c$ the system has outbreak size m. We find that there exist two peaks: one peak at $m = 0$ and the other at $m_u(r) > 0$. This behavior occurs for any r-value above r_a, even though their peak heights depend on r. This result supports the idea that outbreaks need to be categorized into two types: finite and infinite outbreaks. The order parameter is obtained by taking two different types of ensemble average: i) over all samples and ii) over respective samples of finite and infinite outbreaks. The numerical values of $m(r)$ obtained from the two types of averages are denoted as $m_t(r)$ and $m_u(r)$, respectively. As shown in Fig. 7(b), $m_t(r)$ (green •) increase continuously with r. However, data of $m_u(t)$ (orange □) locate on the theoretical curve $m_u(r)$, respectively. The data lying on the line $m \approx 0$ is the average value over finite outbreaks, which is almost zero.

Next, we examine numerically the probability $P_\infty(r)$

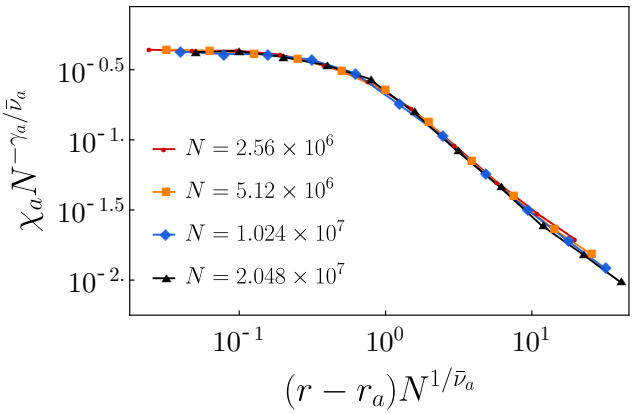

FIG. 6. Scaling plot of the susceptibility χ_a versus the reaction probability r for $r > r_a$ and $\langle k \rangle = 8$. Data are obtained from systems of different system sizes N. With the choice of $\gamma_a = 1$ and $\bar{\nu}_a = 3$, data from different system sizes are well collapsed on a single curve.

that an infinite outbreak occurs in a certain sample, which is proposed as $P_\infty(r) \sim (r - r_a)^{\beta_p}$ with $\beta_p = 1$. By applying finite-size scaling analysis, the probability $P_{\infty,N}(r)$ in finite systems can be written in the scaling form of $P_{\infty,N} \sim N^{-\beta_p/\bar{\nu}_p} g((r - r_a)N^{1/\bar{\nu}_p})$, where $g(x)$ is a scaling function. Indeed in Fig. 8, we find that data for systems of different system sizes N are well collapsed onto a single curve. From this figure, we find that infinite outbreaks rarely occur for $r \ll r_a$, and the probability gradually increases as r approaches r_a in finite systems. As argued in Ref. [10], $P_\infty(r)$ is actually the order parameter of the SIR transition.

We investigate the mean outbreak time of finite outbreaks of size s. The outbreak time is the continu-

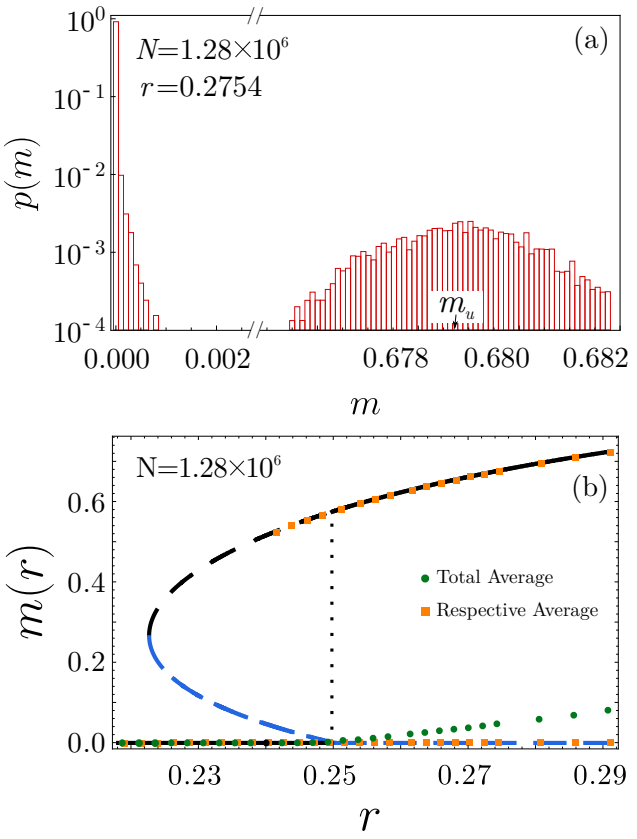

FIG. 7. (a) Plot of the fraction $p(m)$ of the samples having m versus m. The distribution is separated into two curves composed of finite and infinite outbreak samples. (b) Plot of numerical data of $m(r)$ versus r on the theoretical curve shown in Fig. 2. Data are obtained in two different ways, averaged over all samples (green •), over respective finite-outbreak and infinite-outbreak samples (orange □). Data for both (a) and (b) are obtained from systems of $N = 1.28 \times 10^6$ and $\langle k \rangle = 8$.

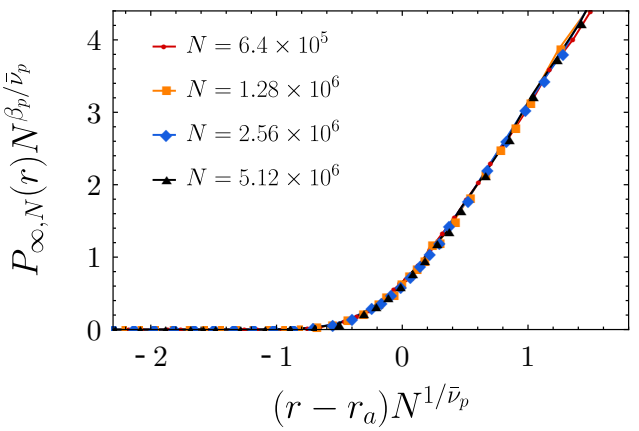

FIG. 8. Scaling plot of rescaled outbreak probability $P_{\infty,N}(r)N^{\beta_p/\bar{\nu}_p}$ that an infinite outbreak occurs in a certain sample versus rescaled reaction probability $\Delta r N^{1/\bar{\nu}_p}$ for $\langle k \rangle = 8$. With the choice of known values $\beta_p = 1$ and $\bar{\nu}_p = 3$, the data are well collapsed onto a single curve.

ous time required to reach an absorbing state. We explain how to calculate a continuous outbreak time in Appendix A. Numerically it is found that $t_{\text{finite}} \sim s^{0.5}$. Using the outbreak size distribution $p_s(r)$ and the relations $p_s ds = p_t dt$ and $s \sim t^2$, we obtain that $p_t(r) \sim t^{-2\tau_a+1} f(t^2/(r-r_a)^{-1/\sigma_a})$. Thus, the mean outbreak time for finite outbreaks scales as $\langle t_{\text{finite}} \rangle \sim -\ln(r - r_a)$ for $r > r_a$ (Fig. 9(a)) and as $\langle t_{\text{finite}} \rangle \sim \ln N$ at $r = r_a$ (Fig. 9(b)).

We remark that the distribution $p_t dt$ can be interpreted as the probability that a spreading epidemic terminates between t and $t+dt$. Then, the surviving probability of the epidemic dynamics surviving up to the time step t is obtained as $q_t = \int p_{t'} dt'$, which is denoted as $q_t \sim t^{-\delta_d}$ following the convention used in the theory of the absorbing phase transition and thus $\delta_d = 2\tau_a - 2 = 1$. Next, the number of nodes (denoted as $u(t)$) that change their state to R at step t averaged over the surviving configurations is obtained by $ds(t)/dt$, which is conventionally denoted as $u(t) \sim t^{\eta_d + \delta_d}$. Thus, $\eta_d = 0$. The exponent values $\eta_d = 0$ and $\delta_d = 1$ are equivalent to the mean field values of the directed percolation universality class [15].

The mean outbreak time of infinite outbreaks differs from that of finite outbreaks. To study the mean outbreak time of infinite outbreaks, we plot the temporal evolution of the order parameter as a function of time for several system sizes in Fig. 10. We numerically obtain that $t_c(N) \sim N^{0.35}$ (Fig. 11). Using the convention for the dynamics exponent z defined as $\xi \sim t^{z/2}$ and the relation $N \sim \xi^d$, where d is spatial dimension, we can say that $2/\bar{z} \approx 0.35$, where $\bar{z} = d_u z$ and d_u is the upper critical dimension, $d_u = 6$ for percolation. This result reveals that the order parameter remains almost unchanged for a long time up to a characteristic time $t_c(N) \approx t_\infty$ beyond which it increases rapidly. Thus, we obtain $\xi \sim \Delta r^{-\nu_\perp}$ with $\nu_\perp = 1/2$ and $t_c \sim (\Delta r)^{-\nu_\parallel}$ with $\nu_\parallel = 1$, where $\Delta r = r - r_a$ [15]. Thus, it is obtained that $z/2 = \nu_\perp = 1/2$ and $2/\bar{z} = 1/3$.

In Ref. [14], it was proposed that a scaling function for the fraction of the nodes in state R of the infinite outbreaks averaged over all configurations is written as $m_t(\Delta r, N, t) = N^{-(\beta_m+\beta_p)/\bar{\nu}_p} m_t(N^{-2/\bar{z}} t, N^{-1/\bar{\nu}_p} \Delta r)$ for $\Delta r \equiv r - r_a > 0$. Here β_m is the order parameter exponent, which is zero for the case $\langle k \rangle > 4$. The factor $N^{-\beta_p/\bar{\nu}_p}$ is derived using the probability that an infinite outbreak occurs in a given sample. The density of the infectious nodes (denoted as ρ_{I}) is obtained as $\rho_{\text{I}}(r, N, t) = \partial_t m(r, N, t)$, which becomes,

$$\rho_{\text{I}}(\Delta r, N, t) = N^{-(\beta_m+\beta_p)/\bar{\nu}_p - 2/\bar{z}} m(N^{-2/\bar{z}} t, N^{-1/\bar{\nu}_p} \Delta r), \tag{19}$$

where the exponents β_m, β_p, $\bar{\nu}_p$ and $\bar{z}$ satisfy the follow-

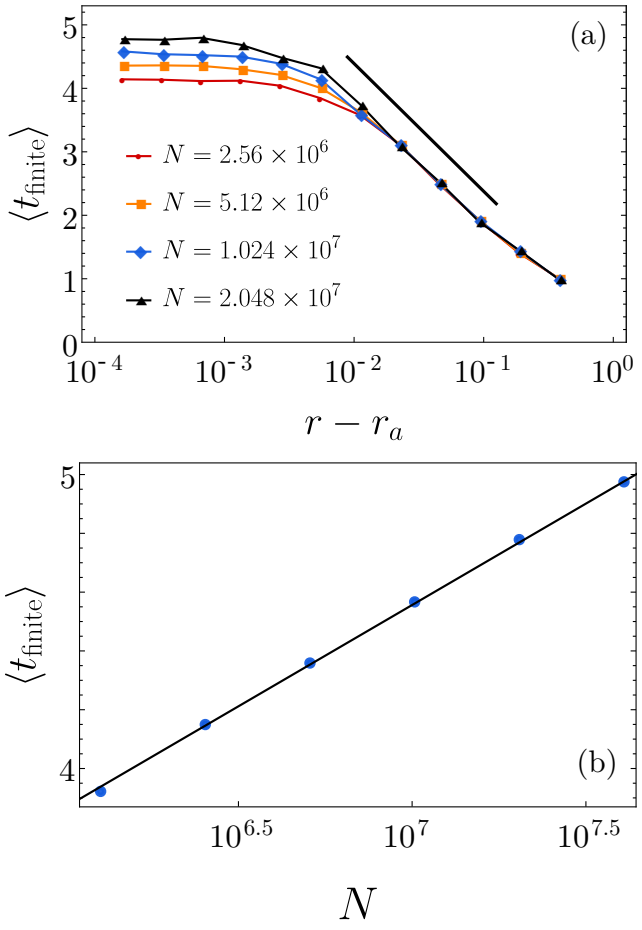

FIG. 9. Plot of the mean outbreak time of finite outbreaks $\langle t_{\rm finite} \rangle$ as a function of (a) $\Delta r = r - r_a$ and (b) N on semilogarithmic scales. Systems of $\langle k \rangle = 8$ are used.

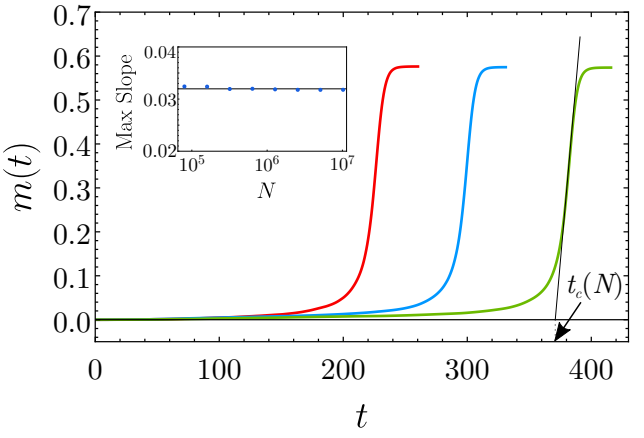

FIG. 10. Plot of temporal evolution of the order parameter as a function of time t for system size $N/10^6 = 2^8, 2^9$ and 2^{10} from left to right for infinite outbreaks. Data are obtained from single trial of the process for each system size with $\langle k \rangle = 8$ at $r = r_a$. Inset: Plot of the mean maximum slope versus N. The slopes show independent behavior of N, indicating that the increase rate of the infinite outbreak size is independent of the system size.

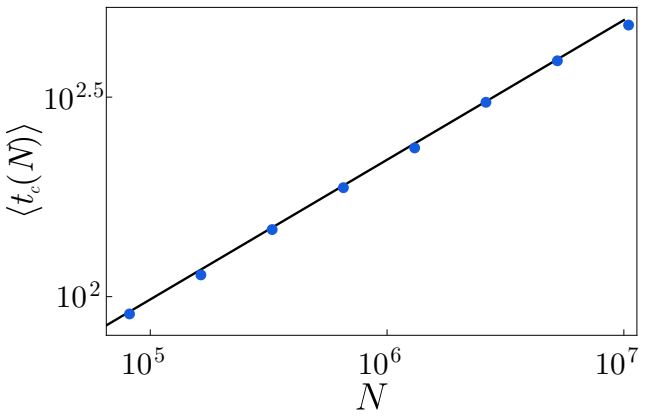

FIG. 11. Plot of the mean outbreak time of infinite outbreaks $\langle t_c(N) \rangle$ versus N on double logarithmic scale. Data are obtained from systems of different system sizes N and $\langle k \rangle = 8$ at $r = r_a$. The guideline has a slope of 0.35.

ing scaling relation.

$$\frac{\beta_m + \beta_p}{\bar{\nu}_p} + \frac{2}{\bar{z}} = 1. \tag{20}$$

Using $\beta_m = 0$, $\beta_p = 1$ and $\bar{\nu}_p = 3$ for percolation, one can obtain $2/\bar{z} = 1 - 1/\bar{\nu}_p = 2/3$. This result is inconsistent with the previous result. This implies that the hyperscaling relation for the case $\langle k \rangle > 4$ does not hold for the MOT.

B. At $\langle k \rangle = 4$

If $\langle k \rangle = 4$, then $r_a = r_b$. Therefore, $a = b = 0$ at $r = r_a$, leading to $b^2 - 4ac = 0$. Thus $r_a = r_*$. For this case, a stable solution of $G(m) = 0$ for $r < r_a$ is $m = 0$. For $r > r_a$, the order parameter behaves as $m(r) = m_u(r) \sim (r - r_a)^{\beta_m}$ with $\beta_m \approx 0.5$, so a continuous phase transition occurs (Fig. 12). In this case, the fluctuations of the order parameter $\chi_m(r) \equiv N(\langle m^2 \rangle - \langle m \rangle^2)$ diverge as $\sim (r - r_*)^{-\gamma_m}$ at $r = r_*$. On the other hand, for the continuous transition, it is not easy to separate the order parameter of $O(N)$ from that of finite outbreaks of $o(N)$ near the transition point. Thus, we determine the exponent γ_m sufficiently far from the transition point. γ_m is measured to be $\gamma_m \approx 1.5$ for $r > r_*$ (Fig. 13).

In such case, the finite-size scaling method is not useful for determining the correlation size exponent $\bar{\nu}_m$ in the critical region. To determine $\bar{\nu}_m$, we used the order parameter defined as $m_t(r) = m(r)P_\infty(r)$ averaged over all samples, which is expected to behave as $\sim (r - r_a)^{\beta_m + \beta_p}$. We confirm in Fig. 14 that the data from different system sizes are well collapsed onto a single curve with the choice of $\beta_m + \beta_p = 1.5$ and $\bar{\nu}_m = 2.5$. Thus, $\bar{\nu}_m \approx 2.5$ is obtained. Thus, we confirm that the hyperscaling relation

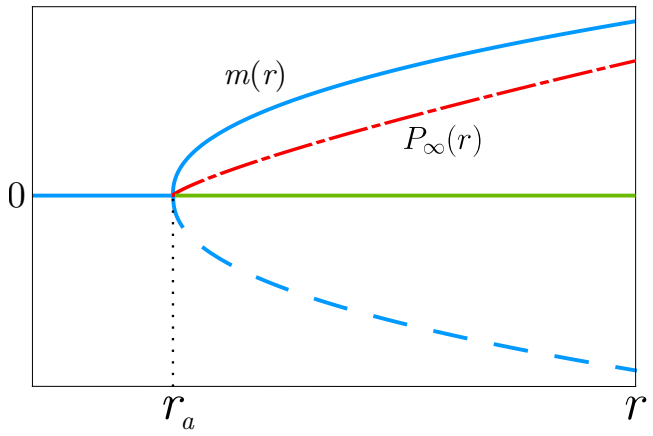

FIG. 12. Schematic plot of the order parameter $m(r)$ as a function of the reaction probability r for the case $\langle k\rangle = 4$. Stable solutions of $m(r)$ are represented by blue (solid) line and curve, whereas unstable solutions are represented by green (solid) line. Physically accessible states are represented by solid lines, whereas inaccessible states are done by dashed lines. The probability $P_\infty(r)$ is indicated by a dashed-dotted curve.

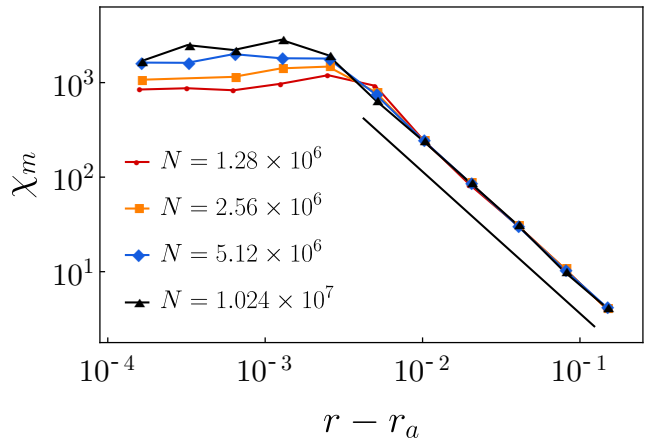

FIG. 13. Plot of the susceptibility χ_m versus the reaction probability for $r > r_a$ and $\langle k\rangle = 4$. Data are obtained from systems of different sizes N. Here, the guideline has a slope of -1.5, which implies that $\gamma_m \approx 1.5$. We remark that data statistics in the plateau region are uncertain because finite and infinite outbreaks are indistinguishable.

$2\beta_m + \gamma_m = \bar{\nu}_m$ holds.

The mean size of finite outbreaks exhibits critical behavior around r_* as $\chi_a = \sum s p_s(r) \sim (r - r_*)^{-\gamma_a}$, where γ_a is measured to be ≈ 1 on both sides of r_* (Fig. 15 and Fig. 16).

The point $(r, m) = (r_a, 0)$ for $\langle k\rangle = 4$ is a tricritical point, because for $\langle k\rangle > (<)4$, the transition is discontinuous (continuous). See also Ref. [14].

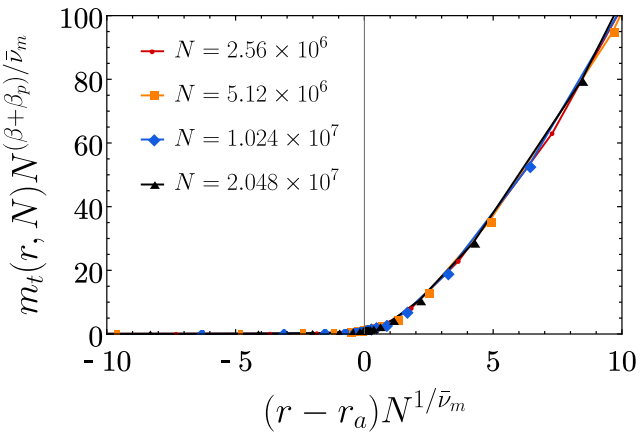

FIG. 14. Data collapse of the order parameter averaged over all configurations in the form of $m_t(r, N)N^{(\beta_m+\beta_p)/\bar{\nu}_m}$ versus $(r - r_a)N^{1/\bar{\nu}_m}$ for $\langle k\rangle = 4$. $\beta_m = 0.5$, $\beta_p = 1$, and $\bar{\nu}_m = 2.5$ are used.

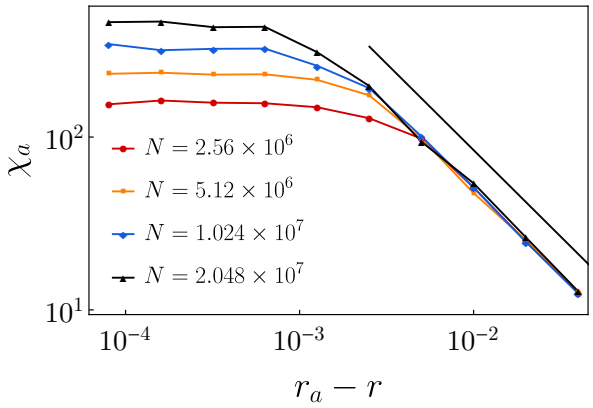

FIG. 15. Plot of the susceptibility χ_a versus the reaction probability $\Delta r = r_a - r$ for the case $\langle k\rangle = 4$. Data are obtained from systems of different sizes N. Here, the guide line has a slope of -1, which implies $\gamma'_a \approx 1$ for $r < r_a$. We remark that the data statistics in the plateau region are uncertain because finite and infinite outbreaks are indistinguishable.

C. For $\langle k\rangle < 4$

When $\langle k\rangle < 4$, $r_b < r_a$. Further, r_* locates between $[r_b, r_a]$ as shown in Fig. 17. At $r = r_*$, $a < 0$, $b > 0$ and $c < 0$, and thus $m_* < 0$. However, for $r > r_a$, the order parameter $m(r) = m_u(r) > 0$, which is physically relevant. The order parameter behaves as $m(r) \sim (r - r_a)$ for $r > r_a$. The fluctuation of the order parameter does not diverge at r_a. On the other hand, the probability $P_\infty(r)$ behaves as $P_\infty(r) \sim (r - r_a)^{\beta_p}$ according to the ordinary percolation theory. The mean size of finite outbreaks χ_a diverges in the critical region around r_a as $\chi_a \sim (r - r_a)^{-\gamma_a}$, where the exponent is measured to be $\gamma_a \approx 1$ for both $r < r_a$ and $r > r_a$ as shown in Fig. 18

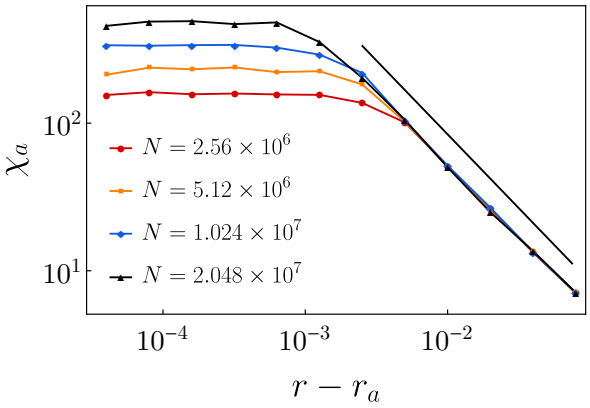

FIG. 16. Plot of the susceptibility χ_a versus the reaction probability $\Delta = r - r_a$ for the case $\langle k \rangle = 4$. Data are obtained from systems of different sizes N. Here, the guideline has a slope of -1, which implies $\gamma_a \approx 1$. We remark that the data statistics in the plateau region are uncertain because finite and infinite outbreaks are indistinguishable.

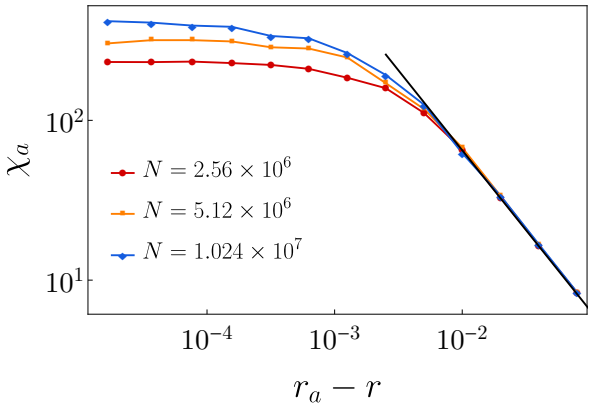

FIG. 18. Plot of the susceptibility χ_a versus the reaction probability $\Delta r = r_a - r$ for $r < r_a$. Data are obtained from systems of different sizes N and $\langle k \rangle = 3$. The guideline has a slope of -1, implying that the susceptibility exponent $\gamma'_a \approx 1.0$. We remark that the data statistics in the plateau region are uncertain because finite and infinite outbreaks are indistinguishable.

and Fig. 19, respectively.

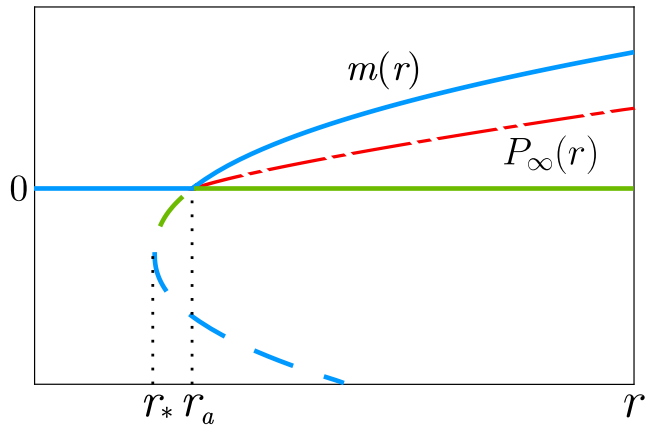

FIG. 17. Schematic plot of the order parameter $m(r)$ as a function of the reaction probability r for the case $\langle k \rangle < 4$. Stable solutions of $m(r)$ are represented by blue (solid or dashed) line and curve, while unstable solutions are done by green (solid or dashed) curve and line. Physically accessible state is represented as solid curve, while inaccessible state is represented as dashed curve. The probability $P_\infty(r)$ is represented by dashed-dotted curve.

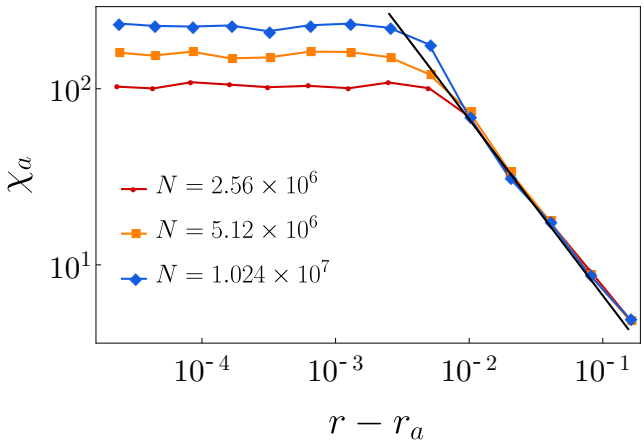

FIG. 19. Plot of the susceptibility χ_a versus the reaction probability $\Delta r = r - r_a$ for $r > r_a$. Data are obtained from systems of different sizes N and $\langle k \rangle = 3$. The guideline has a slope of -1, implying $\gamma_a \approx 1.0$. We remark that the data statistics in the plateau region are uncertain because finite and infinite outbreaks are indistinguishable.

V. SUMMARY AND DISCUSSION

We have investigated critical phenomena occurring in a generalized epidemic spreading model, the SWIR model with single seed [11] on ER random networks with a control parameter, a reaction probability r. The model contains two contagion states, weakened and infected. A susceptible node can be either infected or weakened as it contacts an infectious node. The two cases arise stochastically with respective rate. When mean degree $\langle k \rangle$ is larger than a characteristic value k_c (determined by model parameters), a mixed-order transition (MOT) can occur. The order parameter exhibits a discontinuous jump at a transition point without showing any critical behavior. The fluctuations of the order parameter do not diverge at a transition point. However, other physical quantities such as mean size of finite outbreaks χ_a and the probability $P_\infty(r)$ that an infinite outbreak occurs in a sample exhibit critical behaviors. Thus, the MOT exhibits the feature of continuous and discontinuous transi-

tions at the same transition point. The critical exponents describing the critical behavior of the SWIR model belong to the ordinary percolation universality class. We have analyzed in detail scaling behavior of cascade outbreak dynamics for finite and infinite outbreaks. When mean degree is equal to k_c, a tricritical behavior occurs. The critical exponents for physical quantities at the tricritical point are determined. Finally when $\langle k \rangle < k_c$, a continuous transition occurs. The values of critical exponents for each case are listed in Table I.

The MOTs can be observed in other physical models, for instance, the Ising model in one dimension with long-range interaction following the inverse-square law between two spins within the same domain [20] and a DNA denaturation model [21–23]. In those model systems, the order parameter jumps discontinuously at a transition point without exhibiting critical behavior, whereas the susceptibility and the correlation length diverge, as they appear in the second-order transition.

It would be remarkable that the MOT in the SWIR model differs from the hybrid percolation transition induced by cascading dynamics observed in k-core [24], the cascade failure model on interdependent networks [25] and a generalized epidemic model [16]. For the former, the order parameter does not exhibit any critical behavior, but the outbreak dynamics does. However, for the latter, the order parameter exhibits critical behavior as $m(r) = m_0 + b(r - r_c)^{\beta_m}$ for $r \geq r_c$, where m_0 and b are constants. The fluctuations of the order parameter diverges at r_c. The cascade dynamics exhibits critical behavior as well. It was shown that the underlying mechanism of cascade dynamics is universal for both cases [26].

ACKNOWLEDGMENTS

This work was supported by the National Research Foundation of Korea by grant no. NRF-2014R1A3A2069005.

Appendix A: Simulation rule and determination of epidemic spreading time

During epidemic spreading processes go on, a continuous time variable t passes, which is determined as follows. Suppose that there exists a certain reaction with rate α in the system. Then the probability that the reaction actually occurs between t and $t + dt$ is given as

$$p_1(t)dt = \alpha(1-\alpha)^t dt \approx \alpha e^{-\alpha t} dt. \tag{A1}$$

In our simulations, once we perform the reaction and regard that the reaction occurs at time t_1, which is selected randomly from the probability density function $p_1(t)$. Next, as epidemic spreading proceeds, there exist many possible reactions, e.g., ℓ possible reactions with reaction rates $\{\alpha_1, ..., \alpha_\ell\}$, respectively. Then the probability density function $p(t)$ is given as

$$p(t) = \Big(\sum_j \alpha_j\Big) e^{-t\sum_j \alpha_j}. \tag{A2}$$

Then we perform the reaction j with the probability

$$r_j = \frac{\alpha_j}{\sum_{i=1}^{n} \alpha_i} \tag{A3}$$

and take a time t_i selected randomly from the probability density function (A2). We repeat the above process and obtain times $\{t_1, t_2, \ldots, t_i, \ldots\}$. The final times to reach an absorbing state are given as $t_{\text{finite}} = \sum_i t_i$ and $t_{\text{infinite}} = \sum_i t_i$ for finite and infinite outbreaks, respectively.

Appendix B: Classification of phase transitions

Here we present an analytic method to determine the types of phase transitions as the following cases A-C. Near a certain point (r_x, m_x), we consider the deviation of the function $G(m(r))$ by $\delta G(m)$ as r and m are perturbed by δr and δm, respectively, from (r_x, m_x), and set it to zero.

$$\delta G(r_x, m_x) \simeq \frac{\partial G}{\partial m}\Big|_{r_x,m_x} \delta m + \frac{\partial G}{\partial r}\Big|_{r_x,m_x} \delta r + \frac{1}{2}\frac{\partial^2 G}{\partial m^2}\Big|_{r_x,m_x} (\delta m)^2 + \frac{1}{2}\frac{\partial^2 G}{\partial r^2}\Big|_{r_x,m_x} (\delta r)^2 + \frac{1}{2}\frac{\partial^2 G}{\partial r \partial m}\Big|_{r_x,m_x} (\delta r)(\delta m) + \cdots = 0 \tag{B1}$$

i) For the case $\langle k \rangle > 4$: at $(r_a, m = 0)$, a stable solution exists as $m = 0$. Along this line, the derivatives of all orders are zero, and thus any singular behavior does not occur. Thus, divergent behavior does not occur but a discontinuous transition can occur at $r = r_a$.

TABLE I. List of critical exponents for each type of phase transitions. The values with * are quoted from Ref. [14].

Condition	Type	β_m	γ_m	$\bar{\nu}_m$	τ_a	σ_a	$\bar{\nu}_a$	γ_a
$\langle k\rangle > k_c$	mixed order	0	0	0	1.5	0.5	3	1
$\langle k\rangle = k_c$	tricritical	0.5	1.5	2.5	1.5^*	0.5^*	2.5^*	1
$\langle k\rangle < k_c$	continuous	1	0	0	1.5^*	0.5^*	3^*	1

ii) For the case $\langle k\rangle = 4$: at $(r_a, m = 0)$, $\dfrac{\partial G}{\partial m} = 0$, but $\dfrac{\partial^2 G}{\partial^2 m} < 0$ and $\dfrac{\partial G}{\partial r} > 0$. Thus, $(\delta m)^2 \sim \delta r$. The order parameter behaves $m \sim (r - r_a)^{1/2}$. Thus the transition is continuous with the exponent $\beta_m = 1/2$.

iii) For the case $\langle k\rangle < 4$: at $(r_a, m = 0)$, $\delta m \sim \delta r$, so $\beta_m = 1$.

[1] D. Stauffer and A. Aharony, *Introduction to Percolation Theory* (Taylor & Francis, London; Bristol, PA, 1994).
[2] O. Riordan and L. Warnke, Science **333,** 322 (2011).
[3] Y.S. Cho, S. Hwang, H.J. Herrmann and B. Kahng, Science **339,** 1185 (2013).
[4] G. Bizhani, M. Paczuski, and P. Grassberger, Phys. Rev. E. **86,** 011128 (2012).
[5] Y.S. Cho and B. Kahng, Sci. Rep. **5,** 11905 (2015).
[6] P. Grassberger Math. Biosci. **63** 2, 157 (1983).
[7] M.E.J. Newman Phys. Rev. E **66**, 016128 (2002).
[8] R. Pastor-Satorras, C. Castellano, P. Van Mieghem, and A. Vespignani, Rev. Mod. Phys. **87,** 925 (2015).
[9] L. Chen, F. Ghanbarnejad, W. Cai and P. Grassberger, EPL **104,** 50001 (2013).
[10] W. Cai, L. Chen, F. Ghanbarnejad, and P. Grassberger, Nat. Phys. **11**, 936 (2015).
[11] H.-K. Janssen, M. Müller, and O. Stenull, Phys. Rev. E **70,** 026114 (2004).
[12] T. Hasegawa and K. Nemoto, J. Stat. Mech. P11024 (2014).
[13] P. Erdős and A. Rényi, Publ. Math. **5,** 17 (1960).
[14] K. Chung, Y. Baek, M. Ha and H. Jeong, Phys. Rev. E **93,** 052304 (2016).
[15] J. Marro and R. Dickman, *Nonequilibrium Phase Transitions and Critical Phenomena* (Cambridge University Press, Cambridge, England, 1996).
[16] P. S. Dodds and D.J. Watts, Phys. Rev. Lett. **92,** 218701 (2004).
[17] H.-K. Janssen and O. Stenull, EPL **113,** 26005 (2016).
[18] L. Hébert-Dufresne and B. M. Althouse, PNAS **112** (33), 10551 (2015).
[19] L. Hébert-Dufresne, O. Patterson-Lomba, G. M. Goerg, and B. M. Althouse, Phys. Rev. Lett. **110,** 108103 (2013).
[20] A. Bar and D. Mukamel, Phys. Rev. Lett. **112,** 015701 (2014).
[21] D. Poland and H. A. Scheraga, J. Chem. Phys. **45,** 1456 (1966).
[22] M. E. Fisher, J. Chem. Phys. **45,** 1469 (1966).
[23] Y. Kafri, D. Mukamel, and L. Peliti, Phys. Rev. Lett. **85,** 4988 (2000).
[24] D. Lee, M. Jo and B. Kahng, arXiv:1609.07275.
[25] D. Lee, S. Choi, M. Stippinger, J. Kertesz, and B. Kahng, Phys. Rev. E **93,** 042109 (2016).
[26] D. Lee, W. Choi, J. Kertéz and B. Kahng, arXiv:1608.00776.